Nonradiative and radiative electron capture in collisions of He^+ ions with C atoms below 1000 eV

M. Kimura* and A. Dalgarno
Harvard-Smithsonian Center for Astrophysics, Cambridge, Massachusetts 02138

L. Chantranupong, Y. Li, G. Hirsch, and R. J. Buenker
Theoretische Chemie, Bergische Universität-Gesamthochschule Wuppertal, D-42097 Wuppertal, Germany
(Received 29 October 1993)

Nonradiative and radiative electron captures in collisions of He^+ ions with carbon atoms at energies below 1 keV are studied theoretically by using a molecular-orbital expansion method to calculate the adiabatic potential-energy curves and the nonadiabatic coupling matrix elements of CHe^+. The corresponding scattering equations are solved. For nonradiative transitions, electron capture into channels separating to $He+C^+(^2D)$ are found to be dominant below 10 eV. However, as the energy increases, the channels separating to $He+C^+(^2P)$ take over because of the positive asymptotic energy defect. At 100 eV, the nonradiative capture cross section is 5×10^{-17} cm^2. The radiative electron-capture cross section is found to be very small, with a magnitude nowhere greater than 10^{-22} cm^2.

PACS number(s): 34.70.+e, 34.20.−b, 34.10.+x

I. INTRODUCTION

He^+ ions are produced in planetary ionospheres by the action of extreme ultraviolet radiation, in interstellar clouds by the action of cosmic rays and x rays, and in supernova ejecta by the action of γ rays. He^+ ions, important components of certain fusion plasmas, are removed by radiative and dielectronic recombination and by chemical reactions with molecules. Less certain are reactions of He^+ ions with atoms, because no experimental data exist. Charge transfer, both radiative and nonradiative, of He^+ with H has been studied theoretically over a wide range of energies [1–3], and charge transfer of He^+ with C has been investigated at thermal energies [4]. In this paper we extend the earlier calculations to energies of 1 keV and obtain the cross sections for radiative and nonradiative charge transfer.

II. THEORETICAL MODEL

A. Molecular states

The channels by which electron capture occurs in collisions of He^+ and C are determined by the states of the molecule CHe^+. The electronic states of CHe^+ were investigated by using the multireference single- and double-excitation configuration interaction (MRD-CI) method, with configuration selection and energy extrapolation employing the Table-CI algorithm [5–7]. The carbon atom basis set is of the double-ζ polarization type $(9s5p1d)/[4s2p1d]$ [8], supplemented by the Rydberg functions of $3s$, $3p$, and $3d$ types with exponents $\alpha_s=0.023$, $\alpha_p=0.021$, and $\alpha_d=0.015$. The basis set for the carbon atom may be characterized as $(10s6p2d)/[5s3p2d]$. The helium atom basis set is $(7s)/[5s]$ [9], to which we added a set of polarization functions consisting of two s ($\alpha_s=0.08,0.02$), three p ($\alpha_p=1.0,0.2,0.08$), and one d ($\alpha_d=0.8$) functions onto the helium atom. This basis set for the helium atom may be characterized as $(9s3p1d)/[7s3p1d]$. The configuration selection threshold is $5.0\mu E_h$, and the number of roots treated and the resulting number of generated and selected configurations for each irreducible representation of the C_{2v} point group are given in Table I for a sample bond distance of $2.6a_0$. Table II contains the dominant configurations for each symmetry in energetically increasing order. Some configurations give rise to two roots, as indicated in the table. The multireference analog of the Davidson correction [7] is applied to estimate the full CI energy for each state in the atomic orbital (AO) basis employed. The level of precision of the present asymptotic energies is found from spectroscopic results to be better than 0.1% [10].

For the CHe^+ system, the initial and final capture channels correspond to the

$$[He^+(^2S)+C(^3P):(1\sigma^2 2\sigma^2 3\sigma 1\pi^2)]\ ,$$

$$[He(^1S)+C^+(^2P):(1\sigma^2 2\sigma^2 3\sigma 1\pi^2)]\ ,$$

TABLE I. Number of roots N_{roots} treated in each irreducible representation and the corresponding number of generated F_{SAtot} and selected F_{SAsel} symmetry-adapted functions with a selection threshold of $T=5.0\mu E_h$ at a bond distance of $2.6a_0$.

States	N_{roots}	F_{SAtot}	F_{SAsel}
$^2A_1$	9	144 883	8 160
$^2B_1$	5	141 798	5 248
$^2A_2$	5	153 640	4 021

*Permanent address: Argonne National Laboratory, Argonne, IL 60439 and Department of Physics, Rice University, Houston, TX 77251.

TABLE II. Leading configuration for each of the lowest computed eigenfunctions in energetically increasing order. $(\Sigma+\Delta)$ indicates that both Σ and Δ states originate from the configuration given; the same is true for $(\Pi+\Pi)$ in the case of two Π states.

States	Configurations	
$^2A_1$	$2\sigma^2 3\sigma^2 4\sigma^1$	
	$2\sigma^2 3\sigma^1 1\pi^2$	$(\Sigma+\Delta)$
	$2\sigma^2 3\sigma^2 5\sigma^1$	
	$2\sigma^2 3\sigma^1 4\sigma^2$	
	$2\sigma^2 3\sigma^2 6\sigma^1$	
	$2\sigma^2 3\sigma^2 7\sigma^1$	
	$2\sigma^2 3\sigma^2 8\sigma^1$	
	$2\sigma^2 3\sigma^2 9\sigma^1$	
$^2B_1$	$2\sigma^2 3\sigma^2 1\pi^1$	
	$2\sigma^2 3\sigma^1 4\sigma^1 1\pi^1$	$(\Pi+\Pi)$
	$2\sigma^2 3\sigma^2 2\pi^1$	
	$2\sigma^2 4\sigma^2 1\pi^1$	
$^2A_2$	$2\sigma^2 3\sigma^1 1\pi^2$	$(\Sigma+\Delta)$
	$2\sigma^2 4\sigma^1 1\pi^2$	$(\Sigma+\Delta)$
	$2\sigma^2 3\sigma^2 1\delta^1$	

and

$$[\mathrm{He}(^1S)+\mathrm{C}^+(^2D):(1\sigma^2 2\sigma^2 3\sigma 4\sigma 1\pi)]$$

states, respectively, with respective asymptotic energy defects of $+0.7$ and -3.8 eV. In nonradiative transitions, we expect that the $[\mathrm{He}+\mathrm{C}^+(^2D)]$ state is the larger contributor to electron capture at lower energies and that the $[\mathrm{He}+\mathrm{C}^+(^2P)]$ state will gradually become important as the energy increases. Radiative electron capture may be important below 0.1 eV.

B. Collision dynamics

1. Nonradiative process

To calculate the cross sections for the nonradiative electron-capture processes

$$\mathrm{He}^+(^2S)+\mathrm{C}(^3P)\rightarrow\mathrm{He}(1\,^1S)+\mathrm{C}^+(^2P) \quad (1)$$

and

$$\mathrm{He}^+(^2S)+\mathrm{C}(^3P)\rightarrow\mathrm{He}(1\,^1S)+\mathrm{C}^+(^2D)\ , \quad (2)$$

we employed the molecular-orbital expansion method within a semiclassical framework. Substituting the total wave function, written as a product of electronic wave functions and electron translation factors, into the time-dependent Schrödinger equation, we obtain a set of first-order coupled equations correct to the first order in the relative velocity [11]. By numerically solving the coupled equation, we obtain scattering amplitudes as a function of collision energy E and impact parameter b. The square of the scattering amplitude, a_i, for process i gives a transition probability, and integration of the transition probability over impact parameter gives the cross section. We included six molecular states arising from the initial $(D\,^2\Sigma^-, D\,^2\Pi)$ channels and the final electron capture channels, $[\mathrm{He}+\mathrm{C}^+(^2D)](B\,^2\Pi$ and $B\,^2\Delta)$ and $[\mathrm{He}+\mathrm{C}^+(^2P)](E\,^2\Sigma^-$ and $E\,^2\Pi)$. All of the radial and rotational couplings that connect these states are included in the calculation.

2. Radiative process

For radiative electron capture

$$\mathrm{He}^+(^2S)+\mathrm{C}(^3P)\rightarrow\mathrm{He}(1\,^1S)+\mathrm{C}^+(^2D)+h\nu\ , \quad (3)$$

we used the optical-potential method for radiative transitions [2,12]. In this model, the total probability of radiative electron capture and radiative association per unit time in a radiative transition from the $D\,^2\Pi$ state to the $B\,^2\Pi$ state is described by a complex potential, the imaginary part of which is the spontaneous radiative transition probability at the internuclear distance R. The coupled equation is solved by using a partial-wave decomposition of the amplitude. The imaginary part of the complex phase shift contains the required information on the radiative decay because it measures the loss of photons from each incoming initial channel. The total radiative cross section is given as

$$\sigma=\frac{\pi}{k^2}\sum_J(2J+1)[1-\exp(-4\eta_J)]\ , \quad (4)$$

where η_J is the imaginary part of the complex shift for the Jth partial wave, and k is the wave number of the initial motion.

III. RESULTS

A. Adiabatic potentials and couplings

Figure 1 illustrates the adiabatic potentials for the initial and final capture states. Both initial states, $D\,^2\Sigma^-$ and $D\,^2\Pi$, are attractive, with minima near $R=2a_0$ for $D\,^2\Sigma^-$ and $3.5a_0$ for $D\,^2\Pi$. In contrast, electron-capture states are repulsive except for the $B\,^2\Delta$ state. The initial $D\,^2\Pi$ state undergoes strong avoided crossings with the electron-capture $E\,^2\Pi$ and $B\,^2\Pi$ states at $R=2.1a_0$.

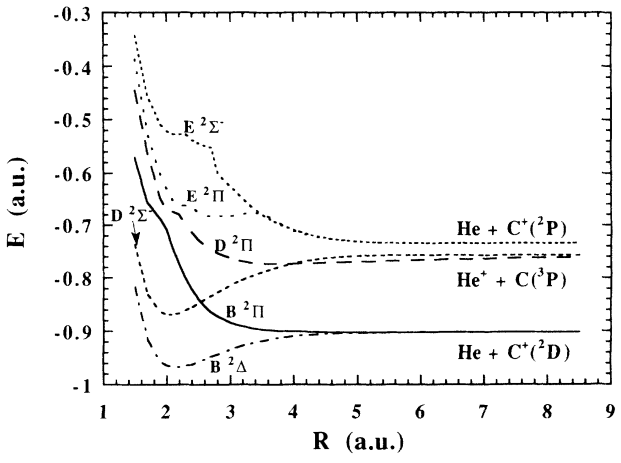

FIG. 1. Adiabatic potential-energy curves of HeC^+.

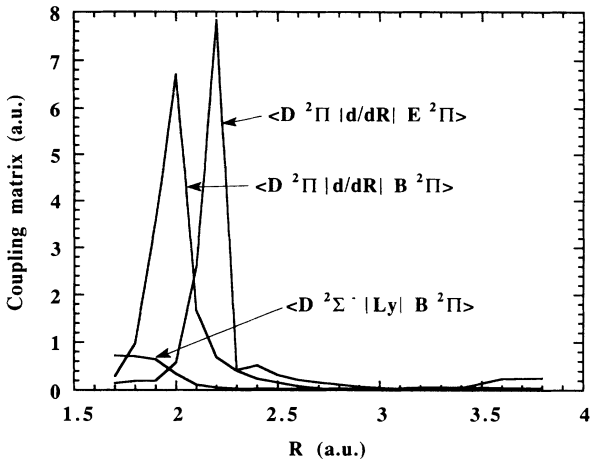

FIG. 2. Representative nonadiabatic coupling matrix elements as functions of R.

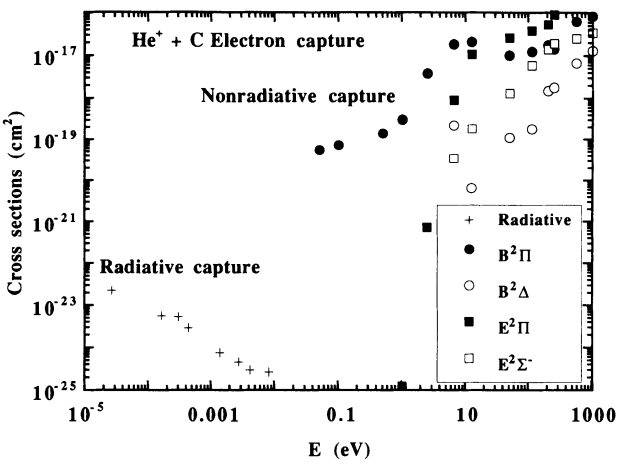

FIG. 4. Nonradiative and radiative electron capture cross sections as functions of the energy E of relative motions.

Hence, these avoided crossings are expected to control the nonradiative electron capture at higher energies. The initial $D\,^2\Sigma^-$ state crosses the $B\,^2\Pi$ state at $R=2.6a_0$, and the rotational coupling that connects these states at the crossing should be dominant for the nonradiative electron-capture dynamics at lower energies, below a few eV. Some representative nonadiabatic coupling matrix elements are displayed in Fig. 2. The Einstein A coefficient for the $D\,^2\Pi \rightarrow B\,^2\Pi$ transition is shown in Fig. 3. Because of strong mixing with nearby states, conspicuous structures appear in the A coefficient.

B. Nonradiative cross sections

The calculated nonradiative electron-capture cross sections for collision energies of 0.1–1000 eV are presented in Fig. 4. As expected from our previous study [4], below 5 eV the $B\,^2\Pi$ state is the sole contributor to electron capture from both the $D\,^2\Sigma^-$ and the $D\,^2\Pi$ initial channels. At much lower energies (below 0.01 eV), the rotational coupling of the $B\,^2\Pi$ state to the $D\,^2\Sigma^-$ is the major mechanism driving the transition [4]. Above 5 eV, the radial coupling of the $E\,^2\Pi$ state to the $D\,^2\Pi$ state becomes dominant, but coupling to the $E\,^2\Sigma^-$ state remains small at all energies. The contribution from the $B\,^2\Delta$ state is small at most energies. The partial cross sections for the $B\,^2\Pi$ and $E\,^2\Pi$ states vary slowly with energy above 8 eV, with a magnitude of 10^{-17} cm^2; those for the $E\,^2\Sigma^-$ and $B\,^2\Delta$ states increase as a function of energy.

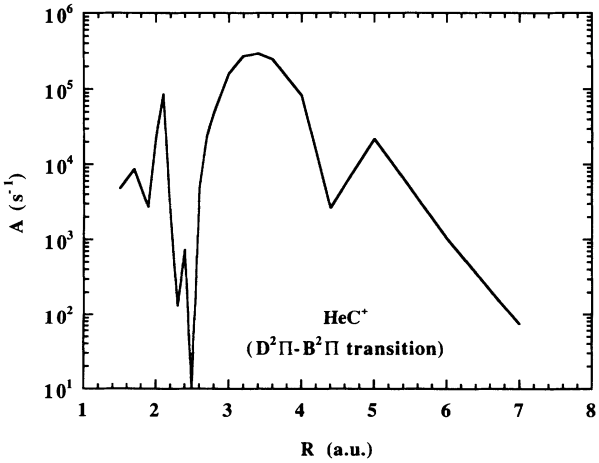

FIG. 3. The Einstein A coefficient for the $D\,^2\Pi \rightarrow B\,^2\Pi$ transition as a function of R.

C. Radiative cross sections

The radiative electron capture cross sections are also shown in Fig. 4. Because of weak dipole coupling, the radiative capture cross section is very small. The overall magnitude of the cross section decreases sharply as the energy increases from 10^{-23} cm^2 at 10^{-4} eV to 10^{-26} cm^2 at 0.1 eV. Several small structures in the cross section are apparent in the energy range studied. These structures are attributed to orbiting resonances of the colliding particles within a van der Waals attractive well. However, the well is very shallow, so that the presence of the structure is weak compared to other systems [2], in which sharp, spikelike peaks have been observed. Because of the small cross sections, this process is unimportant in the dynamics of the collisions of He^+ with C except for energies below 10^{-4} eV, where nonradiative and radiative cross sections are of the comparable order of magnitude.

ACKNOWLEDGMENTS

This work was supported by the U.S. Department of Energy, Office of Health and Environmental Research, Office of Energy Research, under Contract No. W-31-109-Eng-38 (M.K.); by the Office of Basic Energy Science (A.D.); and by the Deutsche Forschungsgemeinschaft (Forschergruppe Th 299/4-2 and Bu 152/12-3) (L.C., Y.L., G.H., and R.B.). M.K. also acknowledges support from the National Science Foundation through the Institute for Theoretical Atomic and Molecular Physics, Harvard University, and the Smithsonian Astrophysical Observatory.

[1] W. Roberge and A. Dalgarno, Astrophys. J. **225**, 489 (1982).
[2] B. Zygelman, A. Dalgarno, M. Kimura, and N. F. Lane, Phys. Rev. A **40**, 2340 (1989).
[3] B. Zygelman and A. Dalgarno, Astrophys. J. **365**, 239 (1990).
[4] M. Kimura, A. Dalgarno, L. Chantranupong, Y. Li, G. Hirsch, and R. J. Buenker, Astrophys. J. **417**, 812 (1993).
[5] R. J. Buenker and S. D. Peyerimhoff, Theor. Chim. Acta **35**, 33 (1974); **39**, 217 (1975); R. J. Buenker, Int. J. Quantum Chem. **29**, 435 (1986).
[6] R. J. Buenker, in *Current Aspects of Quantum Chemistry,* edited by R. Carbo (Elsevier, Amsterdam, 1981), Vol. 21, p. 17; R. J. Buenker and R. A. Phillips, J. Mol. Struct. Theochem. **123**, 291 (1985).
[7] E. R. Davidson, in *The World of Quantum Chemistry,* edited by R. Daudel and B. Pullman (Reidel, Dordrecht, 1974), p. 17; G. Hirsch, P. J. Bruna, S. D. Peyerimhoff, and R. J. Buenker, Chem. Phys. Lett. **52**, 442 (1977); R. J. Buenker, D. B. Knowles, S. N. Rai, G. Hirsch, K. Bhanuprakash, and J. R. Alvarez-Collado, in *Quantum Chemistry—Basic Aspects, Actual Trends,* edited by R. Carbo (Elsevier, Amsterdam, 1989), Vol. 62, p. 181; D. B. Knowles, J. R. Alvarez-Collado, G. Hirsch, and R. J. Buenker, J. Chem. Phys. **92**, 585 (1990).
[8] T. H. Dunning, Jr., J. Chem. Phys. **53**, 2823 (1970).
[9] S. Huzinaga, J. Chem. Phys. **42**, 1293 (1965).
[10] C. E. Moore, *Atomic Energy Levels,* Natl. Bur. Stand. (U.S.) No. 467 (U.S. GPO, Washington, D.C., 1949), Vol. 1.
[11] M. Kimura and N. F. Lane, Adv. At. Mol. Phys. **26**, 79 (1989).
[12] J. S. Cohen and J. N. Bardsley, Phys. Rev. A **18**, 1004 (1978).